Signal-to-noise ratios and spatial frequency spectra of radiographic images of the bone obtained by optical and digital simulation

Ei-ichi Takenaka

From the Department of Radiology (Prof. T. Miyakawa), Faculty of Medicine, University of Tokyo, Japan

(Prof. T. Miyakawa)

Research Code No.: 207

Key Words: *Spatial frequency spectra, S/N, Optical and digital simulation, Bone radiographs, Spatial filtering*

骨X線像の信号対雑音比と空間周波数スペクトル

— ディヂタル計算機及び光学的シミュレーションによる —

東大医学部放射線医学教室

竹　中　栄　一

（昭和46年10月27日受付）

X線映像系における最終提示像はその系の最大空間周波数特性と信号対雑音比（S/N）で定められる．入力情報を調べるため，骨X線像を用い，S/N と空間周波数特性を調べた．前者は光学雑音をマスクして観察能との関係を調べた．その値は平均 7.4 dB であり，100%誤診率，0%誤診率のとき，それぞれ 4.4，16.7 dB である（正規型雑音）．また光学的シミュレーションで視覚的遮断空間周波数を求めた．その値は平均0.53lines/mmであり，計算された空間周波数スペクトル上で，視覚的遮断空間周波数に対する振巾を求めると，平均 6.2%である．この周波数の近傍に診断に重要な details があると考えられる．これらはX線系の設定，像処理，定量診断の基礎的事項として重要である．

1. Preface

In radiologic image transmission systems there are many elements causing noises and influencing image quality; they are X-ray focal spot, intensifying screens, X-ray film and objects to examine (Fig. 1). The maximal transmissible information in X-ray imaging systems is dependent upon signal-to-noise ratios and spatial frequency characteristics of the above-mentioned elements (modulation transfer function, MTF). The spatial frequency spectra (Fourier spectra) of objects must be taken into consideration in order to decide the information necessary to X-ray imaging systems, and in order to know the diag-

Most of this study was reported on the symposium "Some Problems of Radiological Image Quality" at XII ICR in Tokyo, 1969.

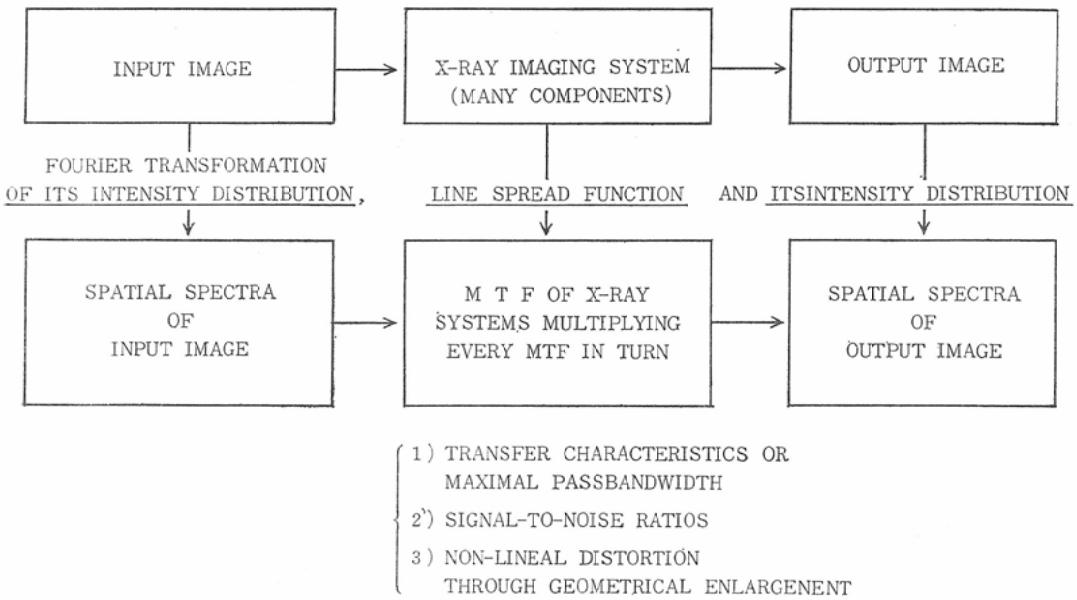

Fig. 1. Spatial frequency and intensity distribution of images and MTF in X-ray imaging systems.

nostically important details of the radiographic images. The information on objects is decided by the following three factors; (1) Physical quantity such as dimension, contrast, signal-to-noise ratios and spatial frequency spectra, (2) psychophysiological quantity such as statistical subjective evaluation or threshold of recognition and (3) physical scales corresponding to the above two factors. There is yet no authorized theoretical treatment with noises in X-ray imaging systems, but the spatial frequency spectra of radiographic images have been obtained by the following methods as digital computer[16], analogue computer[18] and optical transformation[1]. There are few data about the spatial frequency spectra of radiographic images--- or model objects[14][15][16]. We obtained threshold signal-to-noise ratios and visual cutoff frequencies out of spatial frequency spectra of the bone.

2. Threshold S/N of Radiographic Images When Random Noise Charts Used[19][20]

Ten radiologists observed sequences of optically superimposed image pairs on a screen (Fig. 2). Each pair comprised radiographic images and a superimposed random noise image. Five energy levels of projected random noise images of uniform and normal type could be superimposed at one of two energy levels of projected pure radiographic images. Then signal-to-noise ratios (so-called S/N) were measured for various image pairs. Radiologists were then shown features of all image pairs and they were inquired whether they could find out such and such or not. One of three answeres was demanded: "I can...", "Yes, I think I can...", and "No, I cannot...". These were scored as 1, 0.5 and 0, respectively, for three answers to total 25 points about the skull, the femur and the lumbar vertebral bodies (25 point images). S/N on a screen and number of observers who could observe, gave us S/N- observability curves. From these values, the 80 percent observable S/N where eight of ten radiologists could observe images were obtained. The S/N at the probability of completely missing or observing the 25 point images were

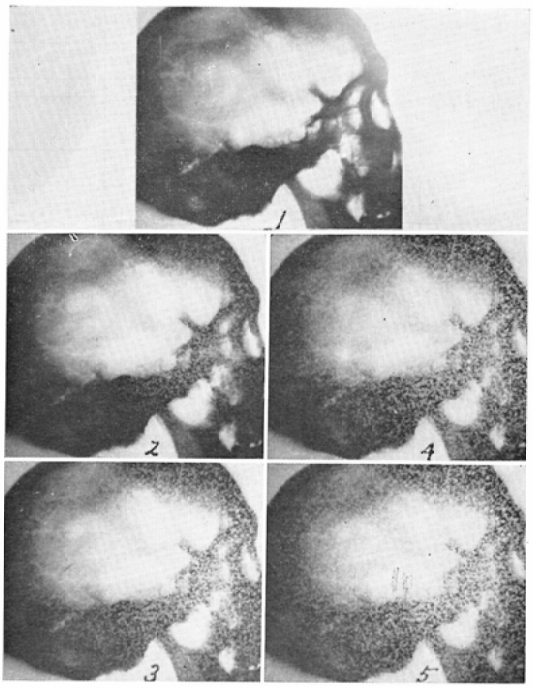

Fig. 2. The observed lateral views of the skull, masked by a random noise chart of uniform type. (Note) 1: No masked; 2, 3, 4 and 5: Illuminations of random noise slide are 3, 7, 15 and 18 lx and illumination of the bone slide is 30 lx.

$$(S/N)=10\ \log_{10}\ (I_s/I_n)$$
$$=10\ \log_{10}\ (S_t/N_t)+10\ \log_{10}\ (I_1/I_2)$$
$$I_s=I_1\times S_r,\ I_n=I_2\times N_t$$

where I_s is a signal illumination; I_n=a noise illumination I_1=an illumination on a screen without projected signal slide; I_2=an illumination on a screen without projected noise slide; St=a transmission factor of signal slide; N_t=an average transmission factor of noise slide.

Corrected S/N is given as followsr:

$$(S/N)_{cor}=10\ \log_{10}\ (A/K)+(S/N)$$

where A is anarea or a length; K=a correction factor. In this papaer K is assumed 1.

Fig. 4. Calculation of S/N and its corrections.

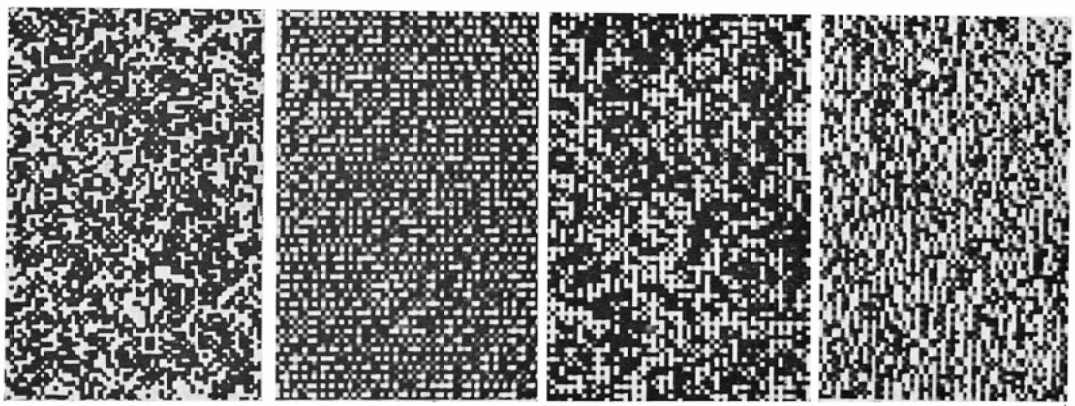

Fig. 3. Four types of random noiste charts.

obtained, from the accumulated percentage points plotted in proportion to the value of the 80 percent observable S/N of the 25 point images (see Fig. 5).

A. Materials, two-dimensional random noise charts, calculation of signal-to-noise ratios and their corrections

As radiographic images, the skull, the femur and the lumbar vertebral bodies were employed. Two-dimensional random noise charts[8][9][10] were used as optical noise sources. These charts correspond to stochastic uniform or normal distribution functions (Fig. 3). These charts have the properties such as excellent reproduciability in every details and availability in any desirable stochastic distribution. Singal-to-noise ratio on a projected screen was given by the ratio of energy of the illumination of a projected radiographic image to that of a projected noise image (Fig. 4). A wide range of value was made by the control of the illumination of signal and noise slides. Corrections for area, length and periodicity where a signal existed were made with thought of increase of S/N because of existence of each factor (Fig. 4).

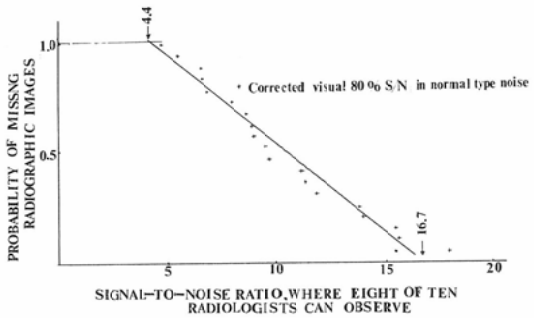

Fig. 5. Probability curve of missing radiographic images of the bone masked by a random chart of normal type.

B. Results and discussion

These objects of the bone had very much low 80 percent observable S/N (Table I). It may be physiological that radiographic images can be observable, although they have such low S/N, compared with televised images[6]. Threshold signal-to-noise ratio reported were in the range oj 2 to 10[3][12][13][14],

Table I　Comparison of the 80 percent observable S/N of the radiographic images of the bone

	Normal type	Uniform type
1. Range	15.5～ 0.5	6.1～—4.9
2. Average without correction	7.4	0.6
3. Average with correction	10.3	3.4
4. At probability of completely a) missing images or b) observing images	4.4 16.7	— 1.3 8.8

Unit: dB

(Note) S/N at the first and second row are uncorrected. S/N at the 4th row are obtained by the method of least squares, using corrected observable S/N.

and these values were calculated by the use of minimal perceptible contrast of simple test objects[2][4][7][11][13][17][21]. From present study, threshold signal-to-noise ratios are shown 0.19～0.13 in the luminance of 300 to 10- foot-lambert[11]. These values are −7.2～−8.8 dB, expressed in decibel units. But this S/N, is not exactly equal to our S/N, and this is thought to be a kind of a clue to the lower limit of observable S/N.

On the contrary, the stationary televised image of a lady drinking coffee, it was said, could not be completely recognized or could be obscured by the signal-to-noise ratio of 20 to 26 dB[6]. But the radiographic images in our experiment were not simple. The corrected observable S/N were nearer to these televised images. If radiographic images must have the same S/N in televised images, the former may have the other correction factor basing on observation conditions. However, it is characteristic that radiographic images have low S/N, we can say. Moreover, supposing that the observable S/N of 25 point images are independent variables, the probability of inability to observe images or missing images is shown in Fig. 5. From Fig. 5, it is seen that radiologists can observe images completely, if radiographic images have the S/N of more than 16.7 dB in normal type. Reversely, radiographic images cannot be observed in less than 4.4. dB in normal type. These values are the lower limit S/N of the corrected 80 percent observable S/N.

3. Spatial Frequency Spectra of Radiographic Images

In order to seek for maximal information of radiographic images, at first the spatial frequency spectra of radiographic images of objects must be known. It is an orthodox method to obtained the spatial frequency spectra by means of fast Fourier transformation[5] of the two-dimensional intensity distribution of complicated radiographic images. The important information is to know the spatial frequency spectra containing diagnostically important details. After all, some part of their spatial spectra can be said to be roentgen-diagnostically necessary. For example, when photographs are blurred to some grade or when their passbandwidths are limited to some spatial frequencies, radiologists become difficult to observe some point in the defocused photographs. Then, the defocused photographs as to some point can be said to have the determined cutoff spatial frequencies. Of course, the accuracy of observation or percentage of observability can be correlated with the defocusing grade of defocused radiographical photographs and it may depend upon the objects themselves and the subjective evaluation of the observers themselves. By the way, these cutoff frequencies or threshold frequency spectra are of very great importance, because we can decide that objects have the special structures proper to themselves around the cutoff frequencies.

A. How to obtain cutoff spatial frequencies

At first, the 4～5 kinds of defocused photographs were reproduced from the pure radiographs used in the S/N threshold experiments. These defocused photographs were made to have the gradually limited passbandwidths and they were photographed with the defocused Siemens' stars, which showed the defocusing levels (Fig. 6). Then, ten radiologists were asked to observe sequences of these optically defocused photographs. Their answers were scored in a similar way to the experiments of visual threshold S/N. These defocused photographs had the cutoff spatial frequencies which were determined by the defocused Siemens' stars, taken together with the photographs. Namely, the threshold of recognizing

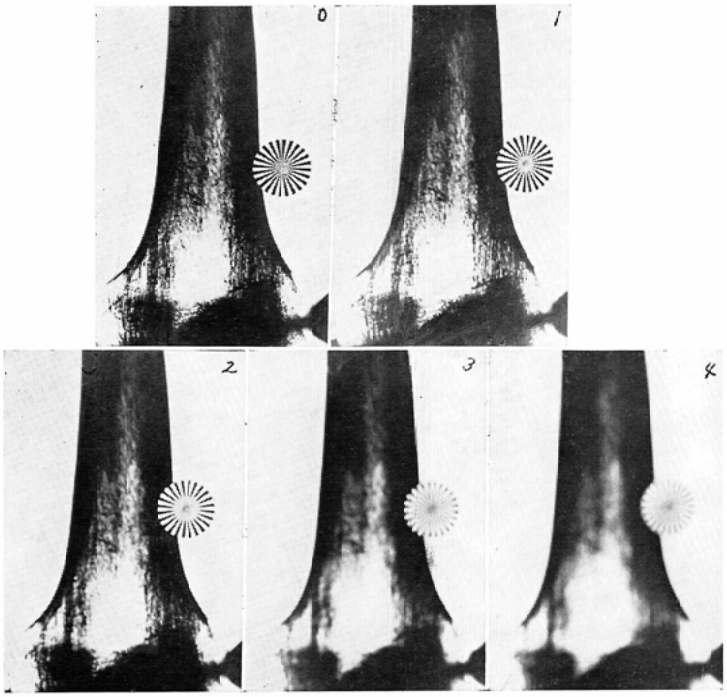

Fig. 6. Several defocused photographs taken from the radiograph of the femur. (Note) "0" is original. The cutoff frequencies of 1, 2, 3 and 4 are 2.5, 1.1, 0.55 and 0.37 lines/mm.

a defocused photograph shows a kind of visual cutoff spatial frequencies of the spatial frequency spectra of the defocused image. These cutoff spatial frequencies are the same as the first cutoff frequencies of defocused Siemens' star. These cutoff frequencies are contained in the diagnostically important spatial spectra extracted from the spatial frequency spectra of radiographic images.

The visual cutoff frequency shows the important details in the intensity distribution of a recognizable area selected out the from intensity distribution of the radiographic images. According to this method, it is simple and easy to obtain the cutoff frequcneies of very much complicated radiographic images, such as the sphenoid sinus, the posterior clinoid process etc. Moreover, these spatial frequency spectra obtained are thought to contain psycho-physiological factors. From this point these cutoff spatial frequencies are more practical than physically calculated frequency spectra.

B. Calculation of spatial frequency spectra of radiographic images and reproduced images with limitation of their passbands (see Appendix)

The spatial spectra of radiographic images with one-dimensional intensity distribution are shown in Fig. 7. The reproduced radiographic images from the spatial frequency spectra were obtained by the use of inverse Fourier transformation. These reproduced images correspond to the transmitted images through the X-ray imaging systems without limitation of passbands. In order to simulate the optically defocused images as shown in Fig. 6, the spatial frequency spectra of radiographic images were limited by means of the function of $(\sin n/g)/n/g$, which was similar to the spatial frequency spectra of the defocusing

Siemens' star. These filtered or limited frequency spectra were inversely Fourier-transformed into the images. From Fig. 7, the hypophyseal fossa had the visual cutoff spatial frequency of 0.17 lines/mm, where its physically calculated spatial spectra had the normalized amplitude of 8.8. And the difference between the original images and the reproduced images with the limited passband of 0.17 lines/mm was about 10 percent. The average amplitude at the visual cutoff frequency as to 25 point images was 6.2%. Most differences between the original images and the passband-limited images were less than 10 percent.

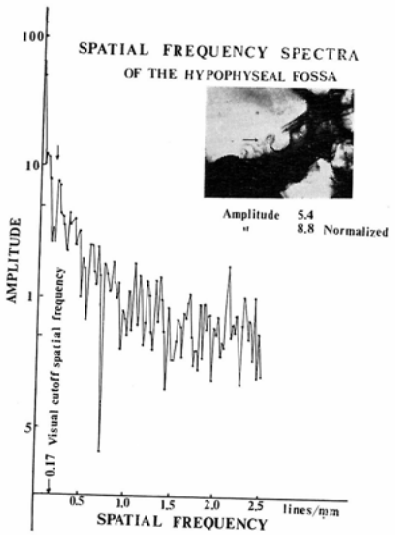

Fig. 7. Spatial frequency spectra of the hypophyseal fossa, calculated by digital computer.

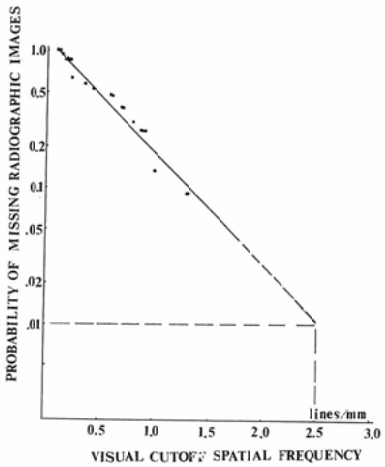

Fig. 8. Probability curve of missing the defocused radiographic images of the bone.

C. Results and discussion

Visual cutoff spatial frequencies obtained were ranged from 0.1 to 1.3 lines/mm and their arithmetic average was 0.53 lines/mm (Table II). Spacious structures had low frequencies, but the suture, the grooves of the meningeal vessels and the trabeculation had the relatively high spatial frequencies. Now, as radiographic photographs are more defocused or as their spatial spectra are limited in narrower passbandwidths, so the image with high frequency components becomes unobservable and then the image with less high components. Finally, even the contour of the image may become unobservable. From the curve of Fig. 8, the probability of missing radiographic images shows that it is difficult physically to obtain a wide passbandwidth so that very fine images can be observable. However the visual cstoff frequency corresponding to the passband may be wide, the probability of missing images can not be zero (Fig. 8). The visual cutoff frequencies were 2.5, 1.7 and 1.3 lines/mm corresponding to the probability of 1, 5 and 10 percent. The radiographic images except the trabeculation had the frequency of about 1.9 lines/mm, when the probability of missing them was 1 percent. The trabeculations of the bone with thin soft tissue such as the fingers, toes and teeth seem to have the very high cutoff frequencies and they seem to be nearly corresponding to the frequency of 3.8 lines/mm, if missing radiographic images are to be permitted one thousandth. These values are helpful to decide the information necessary to X-ray imaging systems and to know the diagnostically important details in radiographic images. For example,

Table Ⅱ Visual cutoff spatial frequency and amplitude of the radiographic images of the bone

	Visual cutoff frequency	Amplitude
1. Range	lines/mm 0.1～ 1.3	1.4～17.3
2. Average	0.53	6.2
3. At probability of a) missing images (100%) or b) observing images (1%)	 0.1 2.5	

Frequencies at the third row are obtained by the method of least squares.

the conventional X-ray television which has the resolution of 1.5 lines/mm or so will not be sufficient from the view point of the visual cutoff frequencies of radiographic images.

The amplitudes of calculated spatial spectra at the visual cutoff spatial frequencies as to 25 point images were normalized with the values of the peak in the neighbourhood of the direct current component and the average amplitude was 6.2. As above-mentioned, the minimal perceptible contrast of simple test objects (see part 2-B) is less than 1 percent. Against this, the average amplitude can be said a clinical minimal perceptible contrast. As cutoff spatial frequency becomes higher, so amplitude there becomes lower.

4. Summary

Signal-to-noise ratios and visual cutoff frequencies of the radiographic images of the bone were studied by the use of optical and digital simulation. Signal-to-noise ratio was 7.4 dB on an average in a normal random noise chart. If the probability of missing radiographic images is 100 or 0 percent, the observable S/N will be 4.4. or 16.7 dB in a normal random noise chart. The visual cutoff spatial frequencies of even complicated radiographic images were simply obtained using optical simulation. They were 0.53 lines/mm on an average. The spatial frequency spectra of the diagnaostically important details must exist around these visual cutoff spatial frequencies. The 1 percent probability of missing radiographic images gives the cutoff frequency of 2.5 lines/mm. The average amplitude of calculated spatial spectra at visual cutoff spatial frequency was 6.2 percent on an average. Those are important to the design of X-ray imaging systems, the processing of radiographic images and quantitative roentgen diagnosis.

Appendix

The Fourier transformation of one-dimensional intensity distribution f(x) of an image is given as follows:

$$F(n) = \int_{-\infty}^{\infty} f(x) \exp(-2n\pi xi)\, dx,$$

where "n" is a spatial frequency (lines/mm). But practical calculations are as follows:

$$F(n) = \int_{a}^{b} f(x) \exp(-2n\pi xi)\, dx$$

$$= \sum_{r=1}^{m} \int_{x_{2r-2}}^{x_{2r}} f(x) \exp(-2n\pi xi)\, dx$$

where the integral interval of a and b is divided in 2m parts and $x_0=a$ and $x_{2m}=b$. The reproduced image of the original is given by means of inverse Fourier transformation of spatial frequency spectra (F(n)).

Reproduced image $$f_{rep}(x) = \int_{-\infty}^{\infty} F(n) \exp(2n\pi xi)\, dn$$

Filtered or limited image $$f_{fil}(x) = \int_{-\infty}^{\infty} F(n) \frac{\sin n/g}{n/g} \exp(2n\pi xi)\, dn$$

Difference $$S = \frac{1}{a-b}\int_a^b \left\{ f_{rep}(x) - f_{fil}(x) \right\} dx$$

where g=parameter.

Acknowledgment: The author is grateful to Prof. T. Miyakawa, K. Kinoshita, D.Sc. and R. Nakajima, B.Sc.

References

1) Becker, H.C., Meyer, P.H. and Nice, C.M.: Digest of VII IC BME (1967), 112.
2) Blackwell, H.R.: Opt. Soc. Am. 36 (1946), 624.
3) Bouwers, A.: From "The diagnostic radiologic instrumentation—modulation transfer function" edited by Moseley, R.D. and Rust, J.H., C.C. Thomas, Illinois. (1965), 90.
4) Coltman, J.W. and Anderson, A.E.: Proc. Inst. Radio Eng. 48 (1960), 858.
5i Cooley, J.W. and Tukey, J.W.: Math. Com. 19 (1965), 297.
6) Dean, C.E.: Proc. IRE (1960 june), 1035.
7) De Palma, J.J. and Lowry, E.M.: J. Opt. Soc. Am. 52 (1962), 328.
8) Fry, G.A.: J. Opt. Soc. Am. 53 (1963), 361., ibid. 53 (1962), 368.
9) Kinoshita, K., Sato, H., Yasuhiro, T. and Ogura, I.: J. Inst. Engr. Jap. (Television), 13 (1959), 434.
10) Kinoshita, K.: Jap. J. Appl. Phys. Suppl., 1 (1964), 215.
11) Morgan, R.H.: Am. J. Roentgenol. 83 (1965), 982.
12) Oosterkampf, W.J.: Acta radiol. suppl. 116 (1954), 497.
13) Rose, A.: J. Opt. Soc. Am. 38 (1948), 196.
14) Rossmann, K.: Radiology 92 (1969), 265.
15) Rossmann, K.: Radiology 90 (1968), 1.
16) Schott, O.: The IIIrd Colloquium diagnostic radiologic instrumen tation in Chicago, 1966.
17) Sturm, R.E. and Morgan, R.H.: Am. J. Roentgenol. 52 (1949), 617.
18) Takenaka, E. and Kinoshita, K.: XII ICR in Tokyo, 1969.
19) Takenaka, E., Kinoshita, K., Sato, H. and Nakajima, R.: Nippon Acta Radiol. 26 (1966), 1249.
20) —ibid. 26, (1967), 1319.
21) Wester, E.W. and Wipfelder, R.: IRE Trans. on Biomedical Electronics. (1962), 150.
22) In this symposium, Schober, H.A.W. reported so, too. Afterthen, Ziskin, M.C. et al. Radiology, 98 (1971), 507, and Rossmann, K. Radiology, 96 (1970), 113, reported.